Alkali Metal Cation π-Interactions in Metalated and Nonmetalated Acetylenes: π-Bonded Lithiums in the X-ray Crystal Structures of $[Li-C{\equiv}C-SiMe_2-C_6H_4-OMe]_6$ and $[Li-O-CMe_2-C{\equiv}C-H]_6$ and Computational Studies

Bernd Goldfuss, Paul von Ragué Schleyer,* and Frank Hampel

Contribution from the Institut für Organische Chemie der Universität Erlangen-Nürnberg, Henkestrasse 42, D-91054 Erlangen, Germany

Received July 2, 1996. Revised Manuscript Received November 4, 1996[⊗]

Abstract: The X-ray crystal structure of $[Li-C{\equiv}C-SiMe_2-C_6H_4-OMe]_6$ (**14**)$_6$ features nearly symmetric π-interactions between the lithium ions and the acetylide anions (Li_1-C_β = 2.353(9) Å, Li_1-C_α = 2.292(9) Å). These π-contacts are facilitated by the chelating *o*-anisyl methoxy groups ($Li_1-C_\alpha-C_\beta$ = 77.6(4)°, Li_1-O_1 = 2.169(9) Å). The $Li-C_\alpha$ distances in the $(LiC_\alpha)_6$ core of (**14**)$_6$ differ significantly ($Li_{1\alpha}-C_\alpha$ = 2.132(9) Å, $Li_{1b}-C_\alpha$ = 2.205(11) Å). This $Li-C_\alpha$ distance differentiation is unique in organolithium hexamers, and is due to $Li(C{\equiv}C-R)$ "side-on-π" and "end-on-σ" contacts, as is shown computationally in $H-C{\equiv}C-Li(LiH)_2$ (**20**). A second X-ray crystal structure, $[Li-O-CMe_2-C{\equiv}C-H]_6$ (**22**)$_6$, reveals electrostatic π-interactions between the lithiums in the $(LiO)_6$ core and the nonmetalated acetylene groups (Li_1-C_2 = 2.443(5) Å, Li_1-C_3 = 2.749(6) Å). These Li−C π-contacts shorten upon acetylene lithiation, as is shown computationally in $Li-O-CH_2-C{\equiv}C-(H/Li)$ (**24-H/Li**). Additional computations reveal that the π-interactions in $(HC{\equiv}C)M_2H$ (**26-Li-Cs**) complexes (modelling oligo- and polymeric $M-C{\equiv}C-R$) are weak (only 0.7 kcal/mol for Li), but substantial in $M^+(H-C{\equiv}C-H)$ (**27-Li-Cs**) species (20.2 kcal/mol for Li^+). In **26-Li-Cs**, the π-contacts increase the C≡C bond lengths slightly (0.005 Å for Li) and lower the C≡C stretching frequencies (33 cm^{-1} for Li), they polarize charge density from C_α toward C_β and hence result in counterion-induced charge delocalizations. The degrees of π-interactions both in (**26-Li-Cs**) and in (**27-Li-Cs**) decrease with increasing size of the alkali cations.

Introduction

In 1976, Apeloig, Schleyer, Binkley, Pople, and Jorgensen discovered computationally that the dilithioacetylene monomer (Li_2C_2) prefers a double π-bridged over a linear structure:[1a]

Li—C≡C—Li

Electrostatic interactions are mainly responsible.[1,2a] This paper is concerned with similar π-interactions both in polar alkali metal acetylides (π-M [M−C≡C−R]) and in nonmetalated acetylenes (π-M [H−C≡C−R]). Such π-interactions are clearly evident in the structures of alkali metal[2] acetylides when the M−C_α and M−C_β distances are similar,[3] e.g., in the polymer sheet arrangements of M−C≡C−H (**1-Na-Rb**)[4] and of M−C≡C−Me (**2-Na-Cs**)[4−6] (Scheme 1, Table 1).

Scheme 1. Polymer Sheet Structure of the Alkali Metal Acetylides **1-Na-Rb** and **2-Na-Cs**[a]

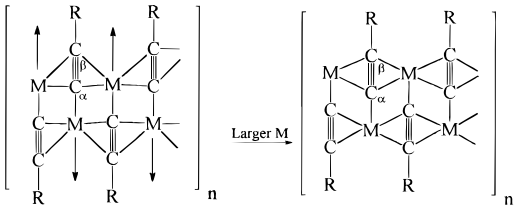

M =	M−C≡C−H	M−C≡C−Me	M−C≡C−Ph
H	**1**	**2**	**13**
Li	**1-Li**	**2-Li**	**13-Li**
Na	**1-Na**	**2-Na**	**13-Na**
K	**1-K**	**2-K**	**13-K**
Rb	**1-Rb**	**2-Rb**	**13-Rb**
Cs	**1-Cs**	**2-Cs**	**13-Cs**
anion	**1-anion**		

[a] The increasing penetration of M−C≡C−R layers with increasing size of M is shown.

However, such metal π-contacts are not always significant; e.g., note the large M−C_β separations (>3 Å) in the oligomeric lithium acetylides: $[(t\text{-}Bu-C{\equiv}C-Li)_4(THF)_4]$ (**3**),[7] [(t-Bu−

⊗ Abstract published in *Advance ACS Abstracts*, January 1, 1997.

(1) (a) Apeloig, Y.; Schleyer, P. v. R.; Binkley, J. S.; Pople, J. A.; Jorgensen, W. L. *Tetrahedron Lett.* **1976**, 3923. (b) Schleyer, P. v. R. *J. Phys. Chem.* **1990**, *94*, 5560. (c) Ritchie, J. P.; Bachrach, S. M. *J. Am. Chem. Soc.* **1987**, *109*, 5909. (d) Jaworski, A.; Person, W. B.; Adamowicz, L.; Bartlett, R. J. *Int. J. Quantum Chem. Symp.* **1987**, *21*, 613.

(2) For reviews on structures of alkali metal organic compounds, see: (a) Sapse, A.-M.; Schleyer, P. v. R., Eds. *Lithium Chemistry*, Wiley: New York, 1995. (b) Lambert, C.; Schleyer, P. v. R. *Angew. Chem.* **1994**, *106*, 1187; *Angew. Chem., Int. Ed. Engl.* **1994**, *33*, 1129. (c) Lambert, C.; Schleyer, P. v. R. *Methoden Org. Chem. (Houben-Weyl)*, 4th ed.; 1952−, Bd. E19d, 1993, p 1. (d) Weiss, E. *Angew. Chem.* **1993**, *105*, 1565; *Angew. Chem., Int. Ed. Engl.* **1993**, *32*, 1501. (e) Gregory, K.; Schleyer, P. v. R.; Snaith, R. *Adv. Inorg. Chem.* **1991**, *37*, 47. (f) Schade, C.; Schleyer, P. v. R. *Adv. Organomet. Chem.* **1987**, *27*, 169. (g) Setzer, W. N.; Schleyer, P. v. R. *Adv. Organomet. Chem.* **1985**, *24*, 353. (h) Bock, H.; Ruppert, K.; Näther, C.; Havlas, Z.; Herrmann, H.-F.; Arad, C.; Göbel, I.; John, A.; Meuert, J.; Nick, S.; Rauschenbach, A.; Seitz, W.; Vaupel, T.; Solouki, B. *Angew. Chem.* **1992**, *104*, 564; *Angew. Chem., Int. Ed. Engl.* **1992**, *31*, 550.

(3) For a discussion of π-interactions in alkaline earth metal acetylides see: Chang, C.-C.; Srinivas, B.; Wu, M.-L.; Chiang, W.-H.; Chiang, M. Y.; Hsiung, C.-S. *Organometallics* **1995**, *14*, 5150.

(4) Weiss, E.; Plass, H. *Chem. Ber.* **1968**, *101*, 2947.

(5) Pulham, R. J.; Weston, D. P. *J. Chem. Res. (S)* **1995**, 406.

(6) Pulham, R. J.; Weston, D. P.; Salvesen, T. A.; Thatcher, J. J. *J. Chem. Res. (S)* **1995**, 254.

S0002-7863(96)02251-2 CCC: $14.00

C≡C−Li)$_{12}$(THF)$_4$],[7] [(Ph−C≡C−Li)tmpda]$_2$ (**4**),[8] and [(Ph−C≡C−Li)$_4$(tmhda)$_{4/2}$] (**5**)[9] (Table 1). In contrast, the short Be−C$_\beta$ distances indicate π-interactions in [(Me−C≡C)$_2$BeNMe$_3$]$_2$ (**6**) (Table 1).[10]

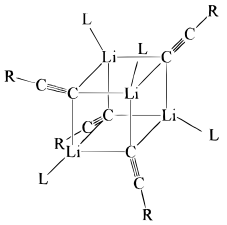

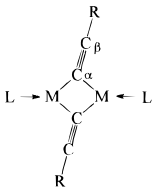

3, R = t-Bu; L = THF
5, R = Ph; L = $^1/_2$tmhda
4, M = Li; R = Ph; L = tmpda
6, M = Be; R = Me; L = (C≡C-Me)(NMe$_3$)

Moreover, the alkali cations in the heterometallic magnesiates Li$_2$[(Ph−C≡C)$_3$Mg(tmeda)]$_2$ (**7**),[11] Na$_2$[(t-Bu−C≡C)$_3$Mg(tmeda)]$_2$ (**8**),[12] and Na$_2$[(t-Bu−C≡C)$_3$Mg(pmdta)]$_2$ (**9**)[12] connect the acetylene moieties of the [Mg(C≡C−R)$_3$]$^-$ fragments through π-contacts (Table 1). Analogous structures as in **7** to **9** result from replacement of M$^+$ by EtMg$^+$ in (Et)(Ph−C≡C)$_3$(Mg)$_2$(tmeda)]$_2$(C$_6$H$_6$) (**10**).[13] Similarly, the lithiums in [Me$_3$SiC(C≡C−t-Bu)$_2$Li]$_2$ (**11**)[2g] as well as the magnesium ion in [(C$_5$HMe$_4$)$_2$Ti(C≡C−SiMe$_3$)$_2$][Mg(THF)Cl] (**12**)[14] are located between the arms of "tweezers" formed by the acetylene groups (Table 1).

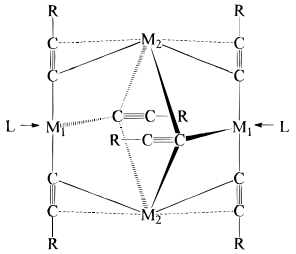

	M$_1$ =	M$_2$ =	R =	L =
7	Mg	Li	Ph	tmeda
8	Mg	Na	t-Bu	tmeda
9	Mg	Na	t-Bu	pmdta
10	Mg	Mg (−Et)	Ph	tmeda

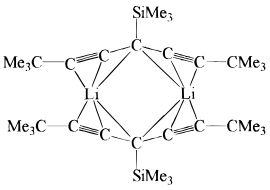

11

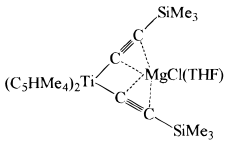

12

How do electrostatic π-interactions affect the electronic structures in metal acetylides? The penetration of the alkali cations into the acetylide layers in **1-Na-Rb** and **2-Na-Cs** increases as the counterions become larger (Scheme 1).[4] The IR ν-C≡C stretching frequencies of **1-Na-Cs**, **2-Li-Cs**, and **13-Li-Cs** decrease with increasing size of the alkali metal cations (Table 2).[15] Negative charge delocalization from C$_\alpha$ to C$_\beta$ is indicated both by the increased metal cation/acetylide interactions upon increased M−C≡C−R layer penetration (see Scheme 1)[4] and by the lower ν-C≡C frequencies.[15] However, an increase in ion size also gives rise to lower ν-C≡C frequencies (see below).[15] How can the effect of π-coordination be differentiated?

Alkali metal π-bonding to benzene ligands has been investigated extensively owing to its important role in biological ion channels.[16] As "lithium-bonded"[17] cyclopropanes emphasize the analogy to hydrogen-bonded cyclopropanes,[17d,18] π-"lithium-bonded" acetylenes stress the analogy to π-hydrogen-bonded acetylenes.[18a,19] The Li$^+$[20] and LiH[21] π-association energies of acetylene are appreciable and are even larger when the acetylenes are metalated.[22] Notwithstanding, Li$^+$ π-bonding has not been observed experimentally in X-ray crystal structures of homogeneous lithium acetylides or in compounds with nonmetalated acetylene groups.[2]

For an assessment of electrostatic metal acetylene π-interactions,[23] we now report the X-ray crystal structures of lithiated (Li−C≡C−SiMe$_2$−C$_6$H$_4$−OMe) and of nonlithiated (Li−O−CMe$_2$−C≡C−H) acetylene moieties. Both exhibit π-bonded Li ions. High level computations reveal the structural, the energetic, and the ω-C≡C vibrational consequences of alkali cation π-interactions in related metal acetylene models and assess the electronic effects of π-coordination.

Results and Discussion

Syntheses and X-Ray Crystal Structures of Homo-Lithium Acetylenes Featuring Electrostatic π-Interactions. Why is π-coordination not apparent in the structures of the oligomeric lithium acetylides **3**, **4**, and **5**? This may be due to (a) insufficient energy gain upon π-bridging (see below), (b) the lower tendency of the smaller alkali metals to undergo multihapto coordination,[2b,c,f] and (c) the competition between the substituents on the acetylene moieties and the lithium coordinating solvent (Scheme 2a).

(7) Geissler, M.; Kopf, J.; Schubert, B.; Weiss, E.; Neugebauer, W.; Schleyer, P. v. R. *Angew. Chem.* **1987**, *99*, 569; *Angew. Chem., Int. Ed. Engl.* **1987**, *26*, 587.
(8) Schubert, B.; Weiss, E. *Chem. Ber.* **1983**, *116*, 3212.
(9) Schubert, B.; Weiss, E. *Angew. Chem.* **1983**, *95*, 499; *Angew. Chem., Int. Ed. Engl.* **1983**, *22*, 496.
(10) Bell, N. A.; Nowell, I. W.; Shearer, H. M. M. *J. Chem. Soc., Chem. Commun.* **1982**, 147.
(11) Schubert, B.; Weiss, E. *Chem. Ber.* **1984**, *117*, 366.
(12) Geissler, W.; Kopf, J.; Weiss, E.; *Chem. Ber.* **1989**, *122*, 1395.
(13) Viebrock, H.; Abeln, D.; Weiss, E. *Z. Naturforsch.* **1994**, *B49*, 89.
(14) Troyanov, S.; Varga, V.; Mach, K. *Organometallics* **1993**, *12*, 2820.
(15) Nast, R.; Gremm, J. *Z. Anorg. Allgem. Chem.* **1963**, *325*, 62.
(16) (a) Mecozzi, S.; West, A. P., Jr.; Dougherty, D. A. *J. Am. Chem. Soc.* **1996**, *118*, 2307. (b) Dougherty, D. A. *Science* **1996**, *271*, 163. (c) Caldwell, J. W.; Kollman, P. A. *J. Am. Chem. Soc.* **1995**, *117*, 4177. (d) Kumpf, R. A.; Dougherty, D. A. *Science* **1993**, *261*, 1708.
(17) (a) Sannigrahi, A. B.; Kar, T.; Niyogi, B. G.; Hobza, P.; Schleyer, P. v. R. *Chem. Rev.* **1990**, *90*, 1061. (b) Scheiner, S. In *Lithium Chemistry*; Sapse, A.-M., Schleyer, P. v. R., Eds.; Wiley: New York, 1995; p 67. (c) Kollman, P. A.; Liebman, J. F.; Allen, L. C. *J. Am. Chem. Soc.* **1970**, *92*, 1142. (d) Goldfuss, B.; Schleyer, P. v. R.; Hampel, F. *J. Am. Chem. Soc.* **1996**, *118*, 12183.
(18) (a) Schleyer, P. v. R.; Trifan, D. S.; Bacskai, R. *J. Am. Chem. Soc.* **1958**, *80*, 6691. (b) Joris, L.; Schleyer, P. v. R.; Gleiter, R. *J. Am. Chem. Soc.* **1968**, *90*, 327. (c) Andrews, A. M.; Hillig, K. W., II; Kuczkowski, R. L. *J. Am. Chem. Soc.* **1992**, *114*, 6765. (d) Buxton, L. W.; Aldrich, P. D.; Shea, J. A.; Legon, A. C.; Flygare, W. H. *J. Chem. Phys.* **1981**, *75*, 2681. (e) Legon, A. C.; Aldrich, P. D.; Flygare, W. H. *J. Am. Chem. Soc.* **1982**, *104*, 1486. (f) Kukolich, S. G. *J. Chem. Phys.* **1983**, *78*, 4832.
(19) (a) Steiner, T.; Tamm, M.; Lutz, B.; Mass, J. v. d. *Chem. Commun.* **1996**, 1127. (b) Allen, F. H.; Howard, J. A. K.; Hoy, V. J.; Desiraju, G. R.; Reddy, D. S.; Wilson, C. C. *J. Am. Chem. Soc.* **1996**, *118*, 4081.
(20) (a) Bene, J. E. D.; Frisch, M. J.; Raghavachari, K.; Pople, J. A.; Schleyer, P. v. R. *J. Phys. Chem.* **1983**, *87*, 73. (b) Dykstra, C. E.; Schaefer, H. F., III *J. Am. Chem. Soc.* **1978**, *100*, 1378.
(21) (a) Houk, K. N.; Rondan, N. G.; Schleyer, P. v. R.; Kaufmann, E.; Clark, T. *J. Am. Chem. Soc.* **1985**, *107*, 2821. (b) Plattner, D. A.; Li, Y.; Houk, K. N. In *Modern Acetylene Chemistry*; Stang, P. J., Diederich, F., Eds.; VCH: Weinheim, 1995; p 1.
(22) Klusener, P. A. A.; Hanekamp, J. C.; Brandsma, L.; Schleyer, P. v. R. *J. Org. Chem.* **1990**, *55*, 1311.
(23) More covalent contributions are apparent in transition metal π-acetylene complexes, e.g.: (a) Chi, K.-M.; Lin, C.-T.; Peng, S.-M.; Lee, G.-H. *Organometallics* **1996**, *15*, 2660. (b) Mingos, D. M. P.; Yau, J.; Menzer, S.; Williams, D. J. *Angew. Chem.* **1995**, *107*, 2045; *Angew. Chem., Int. Ed. Engl.* **1995**, *34*, 1894.

Table 1. M−C_α, M−C_β, and C_α−C_β Distances (Å) in Alkali and Alkaline Earth Metal Acetylenes

	M−C_α[a]	M−C_β	C_α−C_β
M−C≡C−H[b]			
M = Na, **1-Na**	2.49(5)/2.7	3.0	1.17(6)
M = K, **1-K**	2.87/3.0	3.3	1.2
M = Rb, **1-Rb**	2.98/3.2	3.4	1.2
M−C≡C−Me[b]			
M = Na, **2-Na**	2.37(15)/2.7	2.8	1.09(20)
M = K, **2-K**	2.55(5)/3.0	3.1	1.19(6)
(t-Bu−C≡C−Li)$_4$(THF)$_4$, **3**[c]	2.19	>3.1	1.20
[(Ph−C≡C−Li)tmpda]$_2$, **4**[d]	2.13/2.16	3.08	1.24
[(Ph−C≡C−Li)$_4$(tmhda)$_2$], **5**[e]	2.20	>3.1	2.20
[(MeC≡C)$_2$BeNMe$_3$]$_2$, **6**[f]	1.763/2.042	2.538	
Li$_2$[(PhC≡C)$_3$Mg(tmeda)]$_2$, **7**[g]	2.32	2.48	1.22
Na$_2$[(t−Bu−C≡C)$_3$Mg(tmeda)]$_2$, **8**[h,i]	2.571(3)	2.974(3)	1.200(4)
Na$_2$[(t−Bu−C≡C)$_3$Mg(pmdta)]$_2$, **9**[h,i]	2.590(5)	2.900(5)	118.5(7)
[(Et)(PhC≡C)$_3$(Mg)$_2$(tmeda)]$_2$(C$_6$H$_6$), **10**[i,j]	2.265(4)	2.678(4)	1.220(6)
[Me$_3$SiC(C≡C−t−Bu)$_2$Li]$_2$, **11**[k]	2.11	2.34	
[(C$_5$HMe$_4$)$_2$Ti(C≡C−Si]Me$_3$)$_2$][Mg(THF)Cl], **12**[l]	2.269(8)	2.456(9)	1.22(1)
[Li−C≡C−SiMe$_2$−C$_6$H$_4$OMe]$_6$, (**14**)$_6$[m]	2.132(9)/2.205(11)/ 2.292(9)	2.353(9)	1.217(6)

[a] The shorter σ-(M−C_α) and the longer π−(M−C_α) distances are given. [b] Reference 4. [c] Reference 7. [d] Reference 8. [e] Reference 9. [f] Reference 10. [g] Reference 11. [h] Reference 12. [i] Selected bond distances. [j] Reference 13. [k] Reference 2g. [l] Reference 14. [m] See Figure 1.

Table 2. Experimental ν−C≡C Frequencies (cm^{-1}) of Alkali Metal Acetylides (see Scheme 1 for the Structures)

M	M−C≡C−H[a] **1**, **1-Li-Cs**	M−C≡C−Me[a] **2**, **2-Li-Cs**	M−C≡C−Ph[a] **13**, **13-Li-Cs**	**14**
H	1974	2124	2111	2020[b]
Li		2053[c]	2036[d]	1980[c]
Na	1867[e]	2032[c]	2018[c]	
K	1858[c]	2023[c]	2000[c]	
Rb	1851[c]	2020[c]	1990[c]	
Cs	1838[c]	2012[c]	1990[d]	

[a] Reference 15. [b] Neat. [c] Nujol mull. [d] KBr disk. [e] Reference 46.

Scheme 2

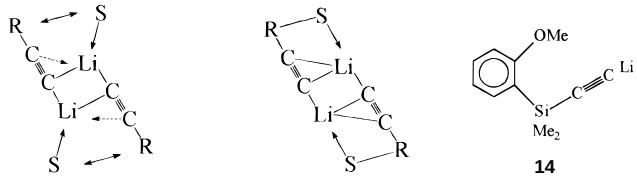

a: Steric competition between the substituent R and the solvent S

b: Lithium-acetylene π-interactions, facilitated by chelation

Recent computations show that solvation by H_2O molecules has sufficient energy to overcome the π-interactions between lithiums and the triple bonds in (**1-Li**)$_2$.[24]

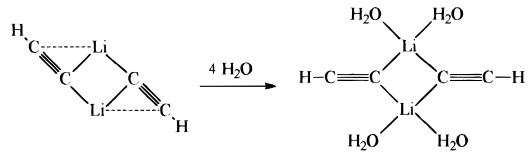

(**1-Li**)$_2$ (**1-Li**)$_2$•4H$_2$O

The goal of this research, to realize a homogenous lithium acetylide exhibiting Li−(C_α≡C_β) π-interactions, as in (**1-Li**)$_2$, without competing external solvent interactions, led us to examine lithium (*o*-anisyl)dimethylsilylacetylide, Li−C≡C−SiMe$_2$−C$_6$H$_4$−OMe (**14**). The *o*-anisyl methoxy group chelation in **14** should result in short Li−C_β contacts (Scheme 2b).

Indeed, the X-ray crystal structure of hexameric **14** (crystallographic S_6 symmetry) shows such nearly symmetric π-interactions; note the short Li−C_β distances in Figure 1 and Table 1.

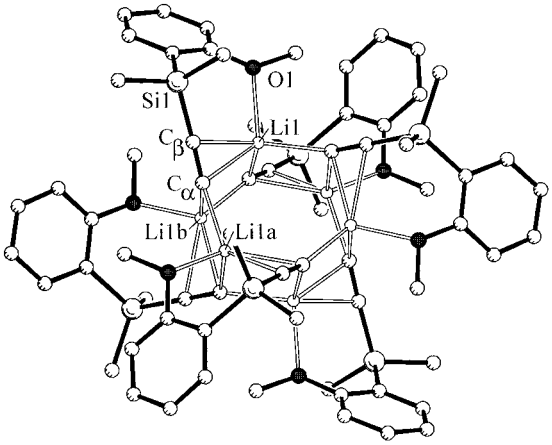

Figure 1. X-ray crystal structure of [Li−C≡C−SiMe$_2$−C$_6$H$_4$−OMe]$_6$ (**14**)$_6$. Hydrogen atoms are omitted. Selected distances (Å) and angles (deg): C_α−C_β, 1.217(6); Li_1−C_α, 2.292(9); Li_1−C_β, 2.353(9); Li_1−O_1, 2.169(9); Li_{1a}−C_α, 2.132(9); Li_{1b}−C_α, 2.205(11); Li_1−C_α−C_β, 77.6(4); Li_{1a}−C_α−C_β, 152.0(5); Li_{1b}−C_α−C_β, 127.8(5).

The lithium ions (Li_1) in (**14**)$_6$ are coordinated 5-fold by three C_α carbon atoms, by the oxygen atoms of the *o*-anisyl methoxy groups (Li_1−O_1: 2.169(9) Å), and by the C_β atoms of the acetylene moieties (Li_1−C_β: 2.353(9) Å, Table 1). The C_α−C_β−Si_1 arrangements (177.8(5)°) are nearly linear. As the C_α≡C_β−R fragments tilt toward Li_1, the $Li_{(1,1a,1b)}$−C_α−C_β angles differ strongly; Li_1−C_α−C_β (77.6(4)°) is much smaller than Li_{1a}−C_α−C_β (152.0(5)°) and the Li_{1b}−C_α−C_β angle is intermediate (127.8(5)°). The C_α≡C_β distances (1.217(6) Å) in (**14**)$_6$ are increased relative to acetylene **1** (exp, 1.20 Å;[25] calc, 1.199 Å; see below). The methyl groups (C_5) on O_1 bend 15° out of the plane of the aryl rings (torsion angle C_5−O_1−C_{66}−C_{62} = −165°).

Comparisons of (**14**)$_6$ and the organolithum hexamers [(c-{C$_6$H$_{11}$}Li)$_6$ (**15**)$_6$•(C$_6$H$_6$)$_2$],[26] [c-{(Me$_2$C)$_2$CH}CH$_2$Li]$_6$ (**16**)$_6$,[27] [Me$_3$SiCH$_2$Li]$_6$ (**17**)$_6$,[28] (n-BuLi)$_6$ (**18**)$_6$,[29] and (i-PrLi)$_6$ (**19**)$_6$[30] are instructive. The (LiC_α)$_6$ cores in all these hexameric

(24) Gareyev, R.; Streitwieser, A. *J. Org. Chem.* **1996**, *61*, 1742.

(25) March, J. *Advanced Organic Chemistry*, Wiley: New York, 1985 and references therein.

(26) Zerger, R.; Rhine, W.; Stucky, G. *J. Am. Chem. Soc.* **1974**, *96*, 6048.

(27) Maercker, A.; Basata, M.; Buchmeier, W.; Engelen, B. *Chem. Ber.* **1984**, *117*, 2547.

(28) Tecle, B.; Rahman, A. F. M. M.; Oliver, J. P. *J. Organomet. Chem.* **1986**, *317*, 267.

Table 3. Bond Distances (Å) and Angles (deg) of the $(LiC_\alpha)_6$ Cores in Hexameric Organolithium Compounds (Scheme 3)

	Li_1-Li_{1a}	$Li_{1a}-Li_{1b}$	Li_1-Li_{1b}	$Li_1-Li_{1b}-Li_{1a}$	α^g	Li_1-C_α	$Li_{1a}-C_\alpha$	$Li_{1b}-C_\alpha$
$[(c\text{-}\{C_6H_{11}\}Li)_6$ (**15**)$_6\cdot(C_6H_6)_2]^a$	2.968	2.397	2.397	74.4	70.3	2.184^h	2.184^h	2.300
$[c\text{-}\{(Me_2C)_2CH\}CH_2Li]_6$, (**16**)$_6{}^b$	2.976	2.462	2.462	76.5	72.2	2.159	2.123	2.297
$[Me_3SiCH_2Li]_6$, (**17**)$_6{}^c$	3.18	2.45	2.45	80.9	79.5	2.20^h	2.20^h	2.28
$(n\text{-}BuLi)_6$, (**18**)$_6{}^d$	2.939	2.429	2.429	74.5	70.3	2.159^h	2.159^h	2.270
$(i\text{-}PrLi)_6$, (**19**)$_6{}^e$	2.959	2.395	2.395	76.3	72.5	2.180^h	2.180^h	2.308
(**14**)$_6{}^f$	3.700	2.794	2.794	82.9	80.5	2.292	2.132	2.205

[a] Reference 26. [b] Reference 27. [c] Reference 28. [d] Reference 29. [e] Reference 30. [f] See Figure 1. [g] Back to seat angle α of the Li_6 chair, Scheme 3b. [h] Average values of similar distances, which do not differ in more than 0.04 Å; see reference.

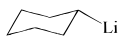

15

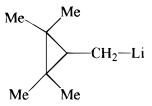

16

organolithium compounds are formed by two stacked $(LiC_\alpha)_3$ rings (Scheme 3a). Folded Li_6 chairs are apparent in the $(LiC_\alpha)_6$ units (Scheme 3b). The C_α atoms cap the Li_3 faces, with one long (Li_1-Li_{1a}) and two short (Li_1-Li_{1b} and $Li_{1a}-Li_{1b}$) distances (Scheme 3c, Table 3).

Relative to (**15**)$_6$, (**16**)$_6$, (**17**)$_6$, (**18**)$_6$, and (**19**)$_6$, the lithium acetylide (**14**)$_6$ exhibits a Li_3 triangle with unusual long Li−Li distances and a rather flat Li_6 chair (large "back-to-seat" angle α, Scheme 3b, Table 3). In (**15**)$_6$ to (**19**)$_6$, the distances of the C_α caps to Li_1 and Li_{1a} are short (Scheme 3c, Table 3). Longer $Li_{1b}-C_\alpha$ distances connect the two stacked $(LiC_\alpha)_3$ rings (Scheme 3a, Table 3). In (**14**)$_6$, however, the Li_1-C_α distances are significantly longer than the $Li_{1b}-C_\alpha$ bonds between the $(LiC_\alpha)_3$ subunits (Table 3).

Our computational model for (**14**)$_6$, H−C≡C−Li(LiH)$_2$ (**20**) (Figure 2), reveals that energy gain upon bending of the $C_\alpha\equiv C_\beta-H$ fragment is low (1.36 kcal/mol in **20**, Figure 2) but that the π-coordination, which results from the tilt of the $C_\alpha\equiv C_\beta-R$ units, gives rise to the unusual $Li-C_\alpha$ distance differentiations in (**14**)$_6$: Shorter σ-$Li-C_\alpha$ (2.027 Å) and longer π-$Li-C_\alpha$ (2.083 Å) distances are apparent in **20-*C*$_s$** relative to **20-*C*$_{2v}$** $Li-C_\alpha$ (2.040 Å, Figure 2). This is due to short "end-on-σ" and long "side-on-π" C_α contacts of the Li ions, which coordinate to the σ- and the π-regions of the acetylide ions (Scheme 4, Figure 3).[2c,b]

Deprotonation or metalation increases the affinity of acetylene groups toward metal ion π-coordination (Figure 4),[22] but the Li^+ and LiH π-interaction energies of nonmetalated acetylene are relatively large (22.2 kcal/mol for π-Li^+(H−C≡C−H); see below).[22,31] The short contacts between lithiums and the carbon atoms in lithium pinacolone enolate $[Li-O-C(t\text{-}Bu){=}CH_2]_6$, (**21**)$_6$ document π-interactions with Li ions in the $(LiO)_6$ cluster (Scheme 5).[32] Are analogous electrostatic π-interactions[33] with (nonmetalated) acetylene moieties possible? To provide an answer, we synthesized and crystallized the lithium acetylene alkoxide $Li-O-CMe_2C\equiv C-H$ (**22**). The X-ray crystal analysis reveals a hexameric aggregate $[Li-O-CMe_2-C\equiv C-H]_6$ (**22**)$_6$ with crystallographic S_6 symmetry (Figure 5).

The lithium centers Li_1 in (**22**)$_6$ exhibit short contacts to the organic moieties (Li_1-C_1 = 2.687(5) Å, Li_1-C_2 = 2.443(5) Å, and Li_1-C_3 = 2.749(6) Å (Scheme 5, Table 4). This suggests similar electrostatic interactions as in (**21**)$_6$ and in $[Li-O-C(Me)-(c\text{-}CHCH_2CH_2)_2]_6$ (**23**)$_6$ (Scheme 5).[17d] This interpretation also is supported by the tilt of the O_1-C_1 moieties toward Li_1 ($Li_1-O_1-C_1$ = 105.3(2)°, $Li_{1a}-O_1-C_1$ = 130.8(2)°, $Li_{1a}-O_1-C_1$ = 134.2(2)°; Table 4) and the coplanarity of the O_1-Li_1 and C_1-C_2 bonds ($Li_1-O_1-C_1-C_2$ dihedral angle = 10.4°, Figure 5).[34] The differences in the $Li_{(1,1a,1b)}$-O_1 distances are remarkable: Li_1-O_1 (1.955(5) Å) are longer than $Li_{1a}-O_1$

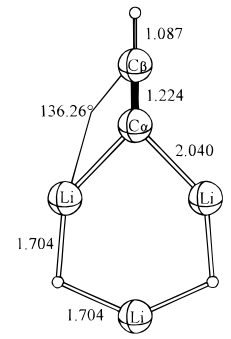

a

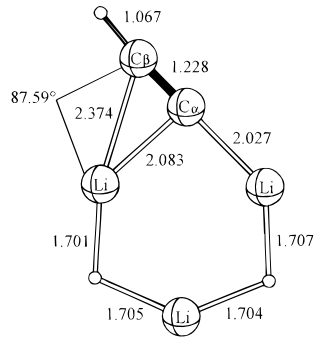

b

Figure 2. (a) H−C≡C−Li(LiH)$_2$ (C_{2v}, **20-C$_{2v}$**): B3LYP/6-311+G** optimized geometry, total energy −100.613 35 au; B3LYP/6-31G* zero-point energy 20.13 kcal/mol (NIMAG = 1). (b) H−C≡C−Li(LiH)$_2$ (C_s, **20-C$_s$**): B3LYP/6-311+G** optimized geometry, total energy −100.61590 au; B3LYP/6-31G* zero-point energy 20.37 kcal/mol (NIMAG = 0); π-coordination energy relative to **20-C$_{2v}$** = 1.36 kcal/mol.

Scheme 3

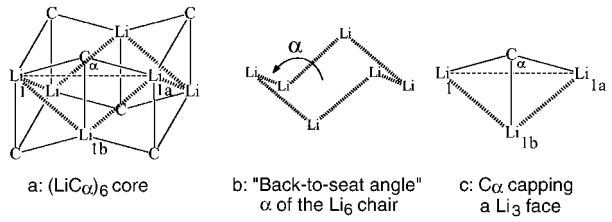

(29) Kottke, T.; Stalke, D. *Angew. Chem.* **1993**, *105*, 619; *Angew. Chem., Int. Ed. Engl.* **1993**, *32*, 580.

(30) Siemeling, U.; Redecker, T.; Neumann, B.; Stammler, H.-G. *J. Am. Chem. Soc.* **1994**, *116*, 5507.

(31) For electrostatic potential computations of H−C≡C−H and F−C≡C−H, see: Clark, D. T.; Adams, D. B. *Tetrahedron* **1973**, *29*, 1887.

(32) (a) Williard, P. G.; Carpenter, G. P. *J. Am. Chem. Soc.* **1985**, *107*, 3345. (b) Williard, P. G.; Carpenter, G. P. *J. Am. Chem. Soc.* **1986**, *108*, 462.

(33) For a discussion of electrostatic Li−C π-interactions in lithium aryls see: Ruhlandt-Senge, K.; Ellison, J. J.; Wehmschulte, R. J.; Pauer, F.; Power, P. P. *J. Am. Chem. Soc.* **1993**, *115*, 11353

(34) Probably due to steric hindrance, ideal syn-periplanar arrangements (Li_1-O_1-C_1-C_2 = 0°) are avoided.

Scheme 4. Differentiation of Li_1-C_α and $Li_{1a}-C_\alpha$ Bonds in the X-ray Crystal Structure of $(\mathbf{14})_6$[a]

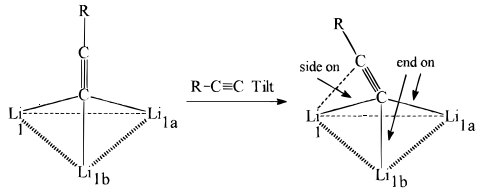

[a] The R−C≡C tilt results in "side-on-π" (Li_1) in addition to the "end-to-σ" (Li_{1a}) coordination. See also Figure 3.

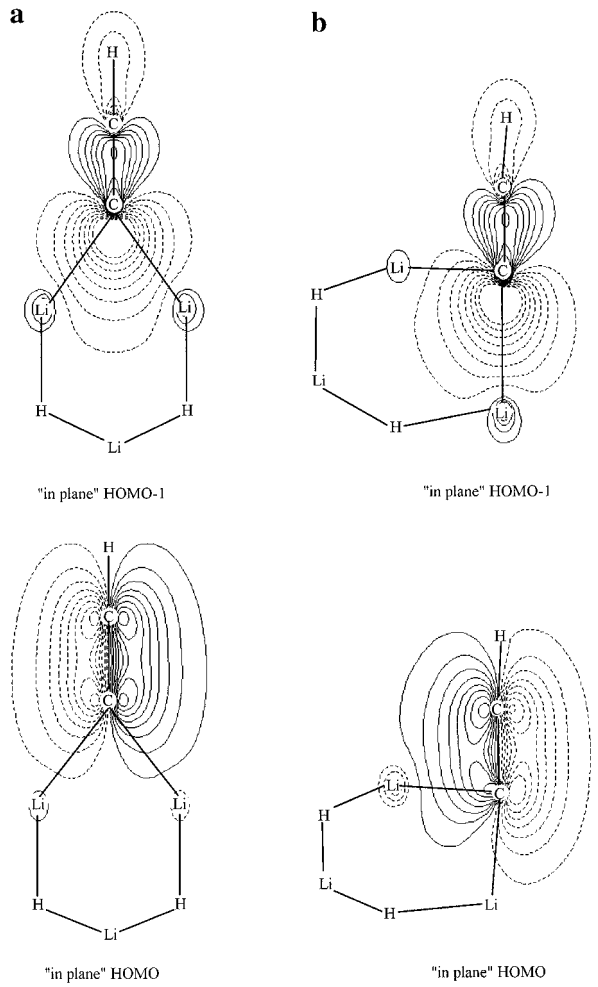

Figure 3. (a) MO contour plots (RHF/6-31+G*) of H−C≡C−Li-$(LiH)_2$ (C_{2v}, **20-C$_{2v}$**) reflecting σ- ("in-plane" HOMO-1) and π- ("in-plane" HOMO) components of the Li−C bonds. (b) MO contour plots (RHF/6-31+G*) of H−C≡C−Li$(LiH)_2$ (C_s, **20-C$_s$**) reflecting σ- ("in-plane" HOMO-1) and π- ("in-plane" HOMO) components of the Li−C bonds.

(1.877(5) Å) or $Li_{1b}-O_1$ (1.923(5) Å). Like the long Li_1-C_α bonds in $(\mathbf{14})_6$, the long Li_1-O_1 distances in $(\mathbf{22})_6$ are obviously due to the "side on p"-coordinated O_1 lone pairs.

To assess the energetics of Li π-bonding in the X-ray crystal structure of $(\mathbf{22})_6$, monomeric Li−O−CH_2−C≡C−H models were computed without (**24-H**, Figure 6a) and with (**24-H-coord**, Figure 6b) Li (H−C≡C) π-contacts (Scheme 6). Both structures are minima. The Li (H−C≡C) π-interaction is rather weak, and **24-H-coord** is only 0.64 kcal/mol more stable than **24-H-coord** (Figure 6, a and b). As in the X-ray crystal structure $(\mathbf{22})_6$, the π-interactions in **24-H-coord** are clearly apparent from the short Li(C≡C) distances (2.241 and 2.478 Å, Figure 6b). Lithiation of the acetylene moiety in **24-H-coord** increases the Li(C≡C) π-interaction in **24-Li-coord** (Figure 4) and results in shorter Li(C≡C) π-contacts (2.115 and 2.290 Å, Figure 6c). Moreover, no minimum corresponding to **24-H** (with X = Li) could be optimized at B3LYP/6-31G*; only **24-Li-coord** resulted.

Structural, Energetic, and Vibrational Effects of π-Interactions in Alkali Metal Acetylides. Similar C_α−M and C_β−M distances (see above) and lower C≡C stretching frequencies are important indicators of π-bonding in polar metal acetylides. Are energetic, structural, and vibrational π-interaction criteria related with the charge distributions in alkali metal acetylides M−C≡C−H (**1-Li-Cs**, Table 5)? The (HC≡C)M_2H complexes correspond to the X-ray crystal structures of **4** and of **6** without (**25-Li-Cs**, C_{2v}) and with (**26-Li-Cs**, C_s) π-interactions (Table 6). Alkali metal cation π-coordinations are apparent in the cationic acetylene complexes **27-Li-Cs** (Table 7).

All C_s structures **26-Li-Cs** with π-interactions are slightly more stable (0.73 kcal/mol (Li) to 0.07 kcal/mol (Cs)) than their C_{2v} counterparts without π-contacts **25-Li-Cs** (Table 6). The C_s-C_{2v} energy differences, ΔE, and hence the degree of π-interaction, decrease with increasing ion sizes (increasing distances r between M^+ and the C≡C centers). This also is apparent with the π-coordination energies E_{coord} of **27-Li-Cs** (Table 7); these correlate with $1/r^3$ (Figure 7).[35] Although **25-Li** and **26-Li** have the largest energy difference, **25-Li** is the only minimum among the C_{2v} species, **25-Li-Cs** (Table 6).[36]

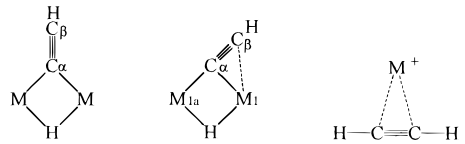

M =	C_{2v}	C_s	C_{2v}
Li	**25-Li**	**26-Li**	**27-Li**
Na	**25-Na**	**26-Na**	**27-Na**
K	**25-K**	**26-K**	**27-K**
Rb	**25-Rb**	**26-Rb**	**27-Rb**
Cs	**25-Cs**	**26-Cs**	**27-Cs**

The C≡C distances elongate as the metal ions become larger in **25-Li** to **25-Cs**, e.g., from 1.225 Å to 1.234 Å, as well as from 1.224 Å in **1-Li** to 1.231 Å ion **1-Cs**, reflecting the σ-effects of the cations in these π-bonding free structures (Tables 5 and 6, Figure 8). The π-interactions in **27-Li** to **27-Cs** (C≡C = 1.205 and 1.201 Å) result only in small C≡C lengthenings relative to **1** (1.199 Å) (Table 7, Figure 8). Similarly, the π-interactions in **26-Li** to **26-Cs** (C≡C = 1.230 and 1.234 Å) elongate the C≡C distances only slightly relative to the corresponding **25-Li-Cs** structures. The C≡C lengthenings due to π-interactions (**25-Li-Cs** vs **26-Li-Cs**) are the greatest the smaller the cations (Figure 8). That the C_α≡C_β distance is a poor criterion for π-interactions has been noted.[3,37]

The σ-coordinated cations shift the harmonic ω-C≡C stretching frequencies to lower values as the metals become larger: from **25-Li** (2007 cm^{-1}) to **25-Cs** (1941 cm^{-1}) and from **1-Li** (2014 cm^{-1}) to **1-Cs** (1955 cm^{-1}, Tables 5 and 6, Figure 9). The π-interactions in **27-Li** to **27-Cs** (ω-C≡C = 2034 and 2053 cm^{-1}) lower the ω-C≡C frequencies relative to **1** (ω-C≡C =

(35) Whereas in alkali metal cation cyclopropane edge complexes E_{coord} depends on $1/r^{2.5}$ (ref 17d), for benzene a $1/r^n$ ($n < 2$) correlation was found (ref 16b).

(36) An earlier computational study using the CCSD/DZP level without diffuse functions describes (HCC)Li_2H as a C_{2v} transition structure: Bolton, E. E.; Laidig, W. D.; Schleyer, P. v. R.; Schaefer, H. F., III *J. Am. Chem. Soc.* **1994**, *116*, 9602.

(37) Tecle, B.; Ilsley, H.; Oliver, J. P. *Inorg. Chem.* **1981**, *20*, 2335.

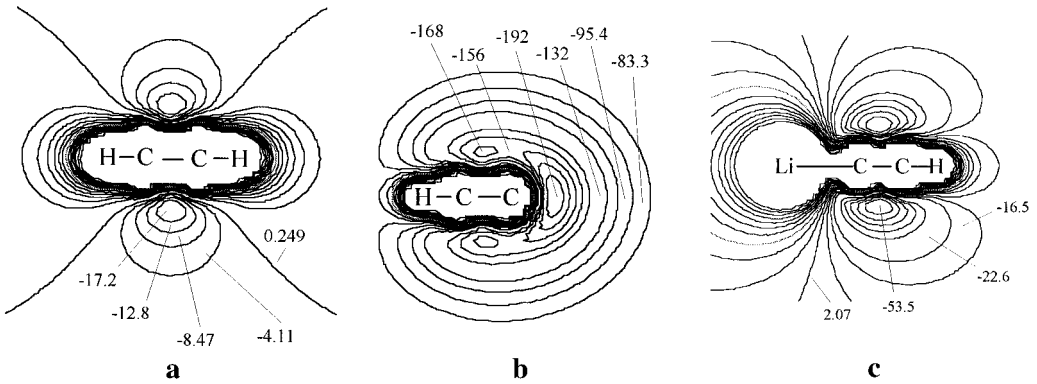

Figure 4. (a−c) Electrostatic potential maps (RHF/6-31+G*) of H−C≡C−H ($D_{\infty h}$, **1**), H−C≡C$^-$ ($C_{\infty v}$, **1-anion**), and Li−C≡C−H ($C_{\infty v}$, **1-Li**). The negative values (kcal/mol) reflect the cation coordination affinities of the systems.

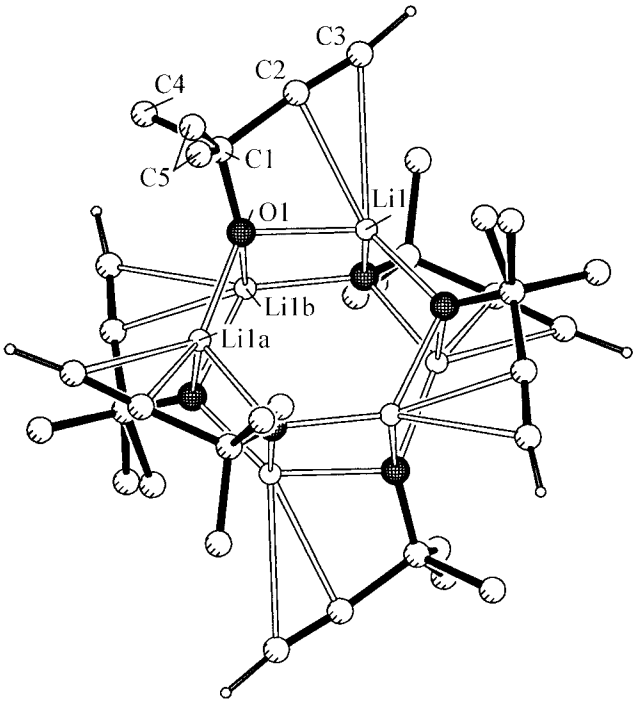

Figure 5. X-ray crystal structure of [Li−O−CMe$_2$−C≡C−H]$_6$ (**22**)$_6$. The methyl groups C$_5$ are disordered. Hydrogen atoms are omitted except the acetylenic hydrogen atom H$_3$. Selected distances (Å) and angles (deg): C$_1$−C$_2$, 1.486(4); C$_2$−C$_3$, 1.172(5); Li$_1$−C$_1$, 2.687(5); Li$_1$−C$_2$, 2.443(5); Li$_1$−C$_3$, 2.749(6); Li$_1$−O$_1$, 1.955(5); Li$_{1a}$−O$_1$, 1.878(5); Li$_{1b}$−O$_1$, 1.932(5); Li$_1$−O$_1$−C$_1$, 105.3(2); Li$_{1a}$−O$_1$−C$_1$, 130.8(2); Li$_{1b}$−O$_1$−C$_1$, 134.2(2).

Scheme 5. Electrostatic Interactions in Hexameric Lithium Alkoxide Clusters

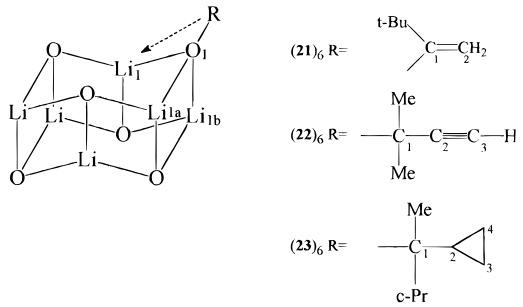

2062 cm^{-1}; Table 7, Figure 9). Similarly, the π-interactions in **26-Li** (1974 cm^{-1}) to **26-Cs** (1937 cm^{-1}) result in lower ω-C≡C stretching frequencies than in the corresponding **25-Li-Cs** structures. The relative reduction of ω-C≡C stretching frequencies (**25-Li-Cs** vs **26-Li-Cs**) is the stronger the smaller the cations and appears as a useful indicator for π-interactions, especially for the smaller cations (Figure 9).

Table 4. Selected Bond Distances (Å) and Angles (deg) for [Li−O−C(t−Bu)=CH$_2$]$_6$, (**21**)$_6$,[a] [Li−O−CMe$_2$−C≡C−H)]$_6$ (**22**)$_6$[b] and [Li−O−C(Me)−(c−CHCH$_2$CH$_2$)$_2$]$_6$ (**23**)$_6$[c] (Scheme 5)

	(**21**)$_6$[a,d]	(**22**)$_6$[b]	(**23**)$_6$[c]
Li$_1$−O$_1$	1.976(9)	1.955(5)	1.937(3)
Li$_{1a}$−O$_1$	1.869(9)	1.877(5)	1.881(3)
Li$_{1b}$−O$_1$	1.954(9)	1.923(5)	1.926(3)
Li$_1$−O$_1$−C$_1$	88.0(9)	105.3(2)	105.6(1)
Li$_{1a}$−O$_1$−C$_1$	140.0(4)	130.8(2)	132.6(1)
Li$_{1b}$−O$_1$−C$_1$	132.9(4)	132.4(2)	135.1(1)
Li$_1$−C$_1$	2.349(9)	2.687(5)	2.680(3)
Li$_1$−C$_2$	2.420(8), 2.53[e]	2.443(5)	2.615(3)
Li$_1$−C$_3$		2.749(5)	2.644(3)

[a] Reference 32. [b] Figure 5. [c] Reference 17d. [d] One of two similar asymmetric units in the unit cell with approximate S_6 symmetry. [e] Average value of the two asymmetric units.

The σ-effects of the cations give rise to increased (C$_\beta$ → C$_\alpha$) charge polarizations with smaller cation sizes in **1-Li-Cs** and in **25-Li-Cs** relative to **1** (see the C$_\alpha$, C$_\beta$ charges in Tables 5 and 6 and in Figure 10). The π-interactions in **26-Li** to **26-Cs** compensate for these counterion induced C$_\alpha$, C$_\beta$ charge separations and hence give rise to C$_\alpha$ → C$_\beta$ charge delocalizations relative to the corresponding **25-Li-Cs** structures. These cation induced charge delocalizations increase with decreasing cation sizes and hence with increasing degrees of the π-interactions (Table 6, Figure 10).

Conclusions

Intramolecular coordination of the *o*-anisyl methoxy groups in [Li−C≡C−SiMe$_2$−C$_6$H$_4$−OMe]$_6$ (**14**)$_6$ eliminates external solvent effects and facilitates lithium π-interactions with the acetylide moieties (Li$_1$−C$_\beta$ = 2.353(9) Å), as is evident in the X-ray crystal structure analysis of (**14**)$_6$. The strong tilt of the C≡C−R fragments in (**14**)$_6$ gives rise to clearly different Li−C$_\alpha$ bond lengths in the (LiC$_\alpha$) core (Li$_1$−C$_\alpha$ = 2.292(9) Å, Li$_{1a}$−C$_\alpha$ = 2.132(9) Å, Li$_{1b}$−C$_\alpha$ = 2.205(11) Å), due to "end-on-σ" and "side-on-π" coordinated acetylide moieties. Such distinct differences in Li−C$_\alpha$ bond distances are unprecedented in the X-ray crystal structures of hexameric organolithium compounds. Similar π-interactions are evident in the X-ray crystal structure of [Li−O−CMe$_2$−C≡C−H]$_6$ (**22**)$_6$ from short distances between the lithium ions in the (LiO)$_6$ cluster and the nonmetalated acetylene moieties (Li$_1$−C$_2$ = 2.443(5) Å, Li$_1$−C$_3$ = 2.749(6) Å). Although the π-contacts are clearly evident structurally, the computational models for the X-ray crystal structures (**14**)$_6$, as well as (**22**)$_6$, H−C≡C−Li(LiH)$_2$ (**20**), and Li−O−CH$_2$−C≡C−H (**24-H**), point to the weak nature of these π-interactions (1.36 and 0.64 kcal/mol, respectively). Further computations

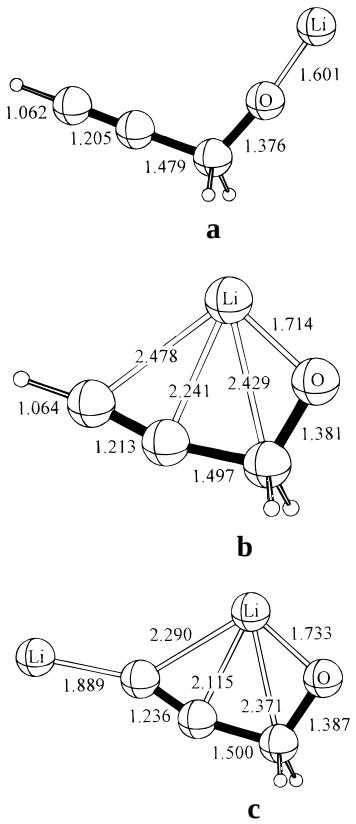

Figure 6. (a) Li−O−CH_2−C≡C−H (C_s **24-H**) without Li (C≡C) π-contacts: B3LYP/6-311+G** optimized geometry, total energy −198.888 99 au; B3LYP/6-31G* zero-point energy 31.91 kcal/mol (NIMAG = 0). (b) Li−O−CH_2−C≡C−H (C_s **24-H-coord**) with Li (C≡C) π-contact; B3LYP/6-311+G** optimized geometry, total energy −198.889 92 au; B3LYP/6-31G* zero-point energy 31.85 kcal/mol (NIMAG = 0); π-coordination energy relative to **24-H** = 0.64 kcal/mol. (c) Li−O−CH_2−C≡C−Li (C_s **24-Li-coord**) with Li (C≡C) π-contact: B3LYP/6-311+G** optimized geometry, total energy −205.829 44 au; B3LYP/6-31G* zero-point energy 26.40 kcal/mol (NIMAG = 0).

Scheme 6. The Li (C≡C) π-Interaction Model for the X-Ray Crystal Structure $(\mathbf{22})_6$ (Figure 6)

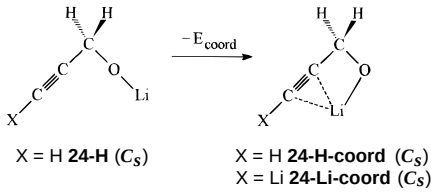

Table 5. Bond Distances (Å),[a] Harmonic Vibrational Frequencies ω (cm^{-1}),[b] and Natural Charges q (aq)[c] of Alkali Metal Acetylides M−C≡C−H

	M−C_α	C_α≡C_β	ω-C≡C	q M	q C_α	q C_β	q H
1 ($D_{\infty h}$)	1.063	1.199	2062		−0.224	−0.224	+0.223
1-Li ($C_{\infty v}$)	1.919	1.224	2014	+0.937	−0.746	−0.386	+0.195
1-Na ($C_{\infty v}$)	2.222	1.225	2002	+0.909	−0.668	−0.436	+0.195
1-K ($C_{\infty v}$)	2.666	1.229	1970	+0.950	−0.643	−0.493	+0.185
1-Rb ($C_{\infty v}$)	2.848	1.230	1964	+0.948	−0.626	−0.506	+0.184
1-Cs ($C_{\infty v}$)	3.057	1.231	1955	+0.961	−0.621	−0.521	+0.182
1-anion ($C_{\infty v}$)		1.243	1882		−0.461	−0.694	+0.155

[a] B3LYP/6-311+G** (C, H), 6-31G (Li, Na), LanL2DZ, ECP (K, Rb, Cs) optimized structures. [b] Unscaled B3LYP frequencies. [c] Natural Population Analysis of the B3LYP electron densities, ref 45.

show the π-interactions in alkali metal (HC≡C)M_2H (**26-Li-Cs**) complexes to be weakly stabilizing (0.73 kcal/mol for Li) and to decrease with increasing cation sizes (0.07 kcal/mol for Cs). The π-contacts give rise to slightly increased C≡C bond lengths (up to 0.005 Å for Li), to lowered ω-C≡C frequencies (up to 33 cm^{-1} for Li) and to cation-induced charge delocalization, which increase with decreasing cation size (Cs to Li).

Experimental Section

The experiments were carried out under an argon atmosphere by using standard Schlenk as well as needle/septum techniques. The solvents were freshly distilled from sodium/benzophenone. Anisole and 2-methyl-3-butyn-1-ol (Aldrich) were distilled prior to use. Sodium acetylide as a toluene/mineral oil suspension and n-BuLi were purchased from Acros. A hexane solution of ^{6}Li-enriched n-Bu^{6}Li was prepared as described by Seebach et al.[38] The NMR spectra were measured on a JEOL GX spectrometer and referenced to TMS or THF: ^{1}H, 400 MHz; ^{13}C, 100.6 MHz; ^{29}Si, 79.4 MHz; ^{6}Li, 58.9 MHz. IR spectra were determined neat or as Nujol mulls between NaCl discs on a Perkin-Elmer 1420 spectrometer. Mass spectral data were obtained on a Varian MAT 311A spectrometer and the elemental analyses (C, H) on Heraeus micro automaton. The X-ray crystal data were collected with an Enraf Nonius CAD4-Mach3 diffractometer using the ω-scan method (3.0° < 2Θ < 54.0°). The structures were solved by direct methods using SHELXS 86. The parameters were refined with all data by full-matrix least-squares on F^2 using SHELXL93 (G. M. Sheldrick, Göttingen, 1993). All nonhydrogen atoms were refined anisotropically; the hydrogen atoms were fixed in idealized positions using a riding model. $R1 = \sum|F_o - F_c|/\sum F_o$ and $wR2 = \sum w|(F_o2 - F_c2)^2|/\sum(w(F_o2)^2)^{0.5}$. Further details are available on request from the Director of the Cambridge Crystallographic Data Center, Lensfield Rd, GB-Cambridge CB2 1 EW, by quoting the journal citation.

Li−C≡C−$SiMe_2$−C_6H_4−OMe (14). A solution of ca. 6.8 g (0.06 mol) *o*-lithioanisole in THF, TMEDA, and hexane was prepared from 37.5 mL (0.06 mol) of BuLi (1.6 M) in hexane, 7.0 g (0.06 mol) of TMEDA, 6.5 g (0.06 mol) of anisole and subsequent solvation of the precipitate with ca. 10 mL of THF.[39] This solution was added dropwise at 0 °C to 7.7 g (0.06 mol) of dichlorodimethylsilane in 150 mL of diethyl ether. The resulting mixture was stirred at room temperature for 6 h and filtered; the volatile components were removed by distillation. The residue was taken up in 150 mL of diethyl ether and cooled to 0 °C; a suspension of 2.9 g (0.06 mol) of sodium acetylide in 20 mL of diethyl ether was added. The mixture was stirred for 6 h at room temperature. Hydrolysis with H_2O/NH_4Cl, extraction with diethyl ether, drying over Na_2SO_4, and distillation yielded (9.8 g, 52 mmol, 87%) *o*-anisyldimethylsilylacetylene, **HC≡C−$SiMe_2$−C_6H_4−OMe**: bp 60 °C/1.6 mbar; ^{1}H NMR ($CDCl_3$) δ 7.69 (d, C_6H_4), 7.35 (t, C_6H_4), 6.97 (t, C_6H_4), 6.79 (t, C_6H_4), 3.76 (s, OCH_3), 2.49 (s, CC*H*), 0.44 (s, $Si(CH_3)_2$); ^{13}C {^{1}H} NMR ($CDCl_3$) δ 165.14, 136.88, 132.40, 124.62, 121.53, 110.48 (C_6H_4), 95.30 (C_α), 89.80 (C_β), 55.92 (O−CH_3), 0.84 ($Si(CH_3)_2$); ^{29}Si {^{1}H} NMR ($CDCl_3$) δ −21.02; IR (neat, cm^{-1}) 3280 (ν C≡C−H); 3070, 3002 (ν C−H arene), 2960, 2900, 2840 (ν C−H aliphatic), 2020 (ν C≡C).

Lithiation of 0.28 g (1.5 mmol) of **HC≡C−$SiMe_2$−C_6H_4−OMe** with 0.9 mL (1.5 mmol) of n-BuLi (1.6 M) in THF or hexane solution (−20 °C, then 5 min. RT) afforded **Li−C≡C−$SiMe_2$−C_6H_4−OMe (14)** (0.27 g, 1.4 mmol, 93% yield in hexane): NMR[40] of ^{6}Li−**14** δ ^{1}H (THF-d_8, +25 °C) 8.13 (d, C_6H_4), 7.24 (t, C_6H_4), 6.88 (t, C_6H_4), 6.77 (d, C_6H_4), 3.74 (s, OCH_3), 0.31 (s, $Si(CH_3)_2$); δ ^{13}C{^{1}H} (THF-d_8, −90 °C) 171.62 (pentuplet, C_α), 164.91 (C_6H_4-OMe), 138.65 (C_6H_4), 131.27 (C_6H_4), 127.04 (C_6H_4-$SiMe_2$), 120.25 (C_6H_4), 114.23 (s, C_β), 109.11 (C_6H_4), 55.00 (OCH_3), 0.97 ($Si(CH_3)_2$); δ ^{6}Li (THF-d_8, −95 °C) −0.26 (s); δ ^{29}Si {^{1}H} (THF-d_8, 31 °C) −30.55; IR (Nujol, cm^{-1}) 3050 (ν C−H arene), 1980 (ν C≡C); MS (EI, 70 eV, 120 °C) *m/e* 354 [Me−O−C_6H_4−$SiMe_2$−C≡C−$SiMe_2$−C_6H_4−OMe]$^+$, 339 [Me−O−C_6H_4−$SiMe_2$−C≡C−SiMe−C_6H_4−OMe]$^+$, 324 [Me−O−C_6H_4−SiMe−C≡C−SiMe−C_6H_4−OMe]$^+$, 309 [Me−O−C_6H_4−Si−C≡C−SiMe−C_6H_4−OMe]$^+$, 294 [Me−O−C_6H_4−Si−C≡C−Si−C_6H_4−OMe]$^+$, 279

(38) Seebach, D.; Hässig, R.; Gabriel, J. *Helv. Chim. Acta* **1983**, *66*, 308.

(39) Brandsma, L.; Verkruijsse, H. *Preparative Polar Organometallic Chemistry*; Springer: Berlin 1987.

(40) For NMR [^{6}Li ^{13}C] coupling studies on lithium acetylides see: (a) Fraenkel, G.; Pramanik, P. *J. Chem. Soc., Chem. Commun.* **1983**, 1527. (b) Hässig, R.; Seebach, D. *Hev. Chim. Acta* **1983**, *66*, 2269.

Table 6. Energies,[a] Bond Distances (Å),[a] Harmonic Vibrational Frequencies ω (cm^{-1}),[b] and Natural Charges q (au)[c] of ($HC{\equiv}C)M_2H$ Complexes without (C_{2v}) and with (C_s) π-Interactions

	E, ZPE (NIMAG)[d]	ΔE[e]	M_1-C_α	$M_{1a}-C_\alpha$	$M-C_\beta$	$C_\alpha{\equiv}C_\beta$	ω-C≡C	q M[f]	q C_α	q C_β	q H
25-Li (C_{2v})	−92.445 65, 15.79 (0)		2.091	2.091	3.183	1.225	2007	+0.873	−0.775	−0.337	+0.204
26-Li (C_s)	−92.446 81, 15.79 (0)	0.73	2.126	2.051	2.446	1.230	1974	+0.874	−0.652	−0.478	+0.213
25-Na (C_{2v})	−401.966 01, 14.03 (1, −79)		2.415	2.415	3.484	1.227	1983	+0.878	−0.703	−0.409	+0.199
26-Na (C_s)	−401.967 15, 14.10 (0)	0.65	2.428	2.389	2.929	1.230	1968	+0.879	−0.642	−0.477	+0.202
25-K (C_{2v})	−133.658 25, 12.95 (1, −44)		2.834	2.834	3.860	1.231	1956	+0.923	−0.658	−0.487	+0.192
26-K (C_s)	−133.658 69, 13.02 (0)	0.21	2.838	2.836	3.416	1.233	1950	+0.923	−0.621	−0.523	+0.193
25-Rb (C_{2v})	−125.102 71, 12.60 (1, −45)		3.025	3.005	4.035	1.232	1948	+0.924	−0.637	−0.508	+0.190
26-Rb (C_s)	−125.103 08, 12.67 (0)	0.16	3.031	3.033	3.595	1.232	1942	+0.923	−0.607	−0.537	+0.191
25-Cs (C_{2v})	−117.125 51, 12.35 (1, −41)		3.229	3.229	4.217	1.234	1941	+0.937	−0.626	−0.529	+0.188
26-Cs (C_s)	−117.125 74, 12.42 (0)	0.07	3.232	3.243	3.835	1.234	1937	+0.936	−0.605	−0.549	+0.188

[a] B3LYP/6-311+G** (C, H), 6-31G (Li, Na), LanL2DZ, ECP (K, Rb, Cs) optimized structures. [b] Unscaled B3LYP frequencies. [c] Natural Population Analysis of the B3LYP electron densities, ref 45. [d] Total energies E (au), unscaled zero-point energies ZPE (kcal/mol), numbers and values (cm^{-1}) of imaginary frequencies in parentheses. [e] Relative C_s-C_{2v} energies ΔE (kcal/mol). [f] Average value for M_1 and M_{1a}.

Table 7. The π- Coordination Energies E_{coord} (kcal/mol),[a] Bond Distances (Å),[a] Harmonic Vibrational Frequencies ω (cm^{-1}),[b] and Natural Charges q (au)[c] of the Alkali Cation Acetylene Complexes $M^+(H-C{\equiv}C-H)$

	E_{coord}	M^+ $\pi-(C{\equiv}C)$[d]	$C_\alpha{\equiv}C_\beta$	$\omega-C{\equiv}C$	q M	q C	q H
1 ($D_{\infty h}$)			1.199	2062		−0.223	+0.223
27-Li (C_{2v})	20.22	2.254	1.205	2034	+0.978	−0.261	+0.272
27-Na (C_{2v})	13.29	2.633	1.204	2039	+0.986	−0.252	+0.259
27-K (C_{2v})	7.50	3.152	1.202	2048	+0.997	−0.245	+0.246
27-Rb (C_{2v})	5.73	3.454	1.201	2051	+0.998	−0.241	+0.242
27-Cs (C_{2v})	4.53	3.739	1.201	2053	+0.999	−0.238	+0.239

[a] B3LYP/6-311+G** (C, H), 6-31G (Li, Na), LanL2DZ, ECP (K, Rb, Cs) optimized structures. [b] Unscaled B3LYP frequencies. [c] Natural Population Analysis of the B3LYP electron densities, ref 45. [d] Distance between the metal and the center of the C≡C bond.

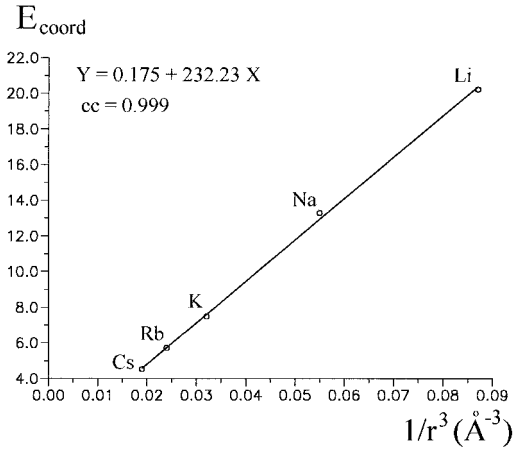

Figure 7. The $1/r^3$ dependence of the coordination energy E_{coord} in M^+ ($H-C{\equiv}C-H$) complexes (**27-Li-Cs**).

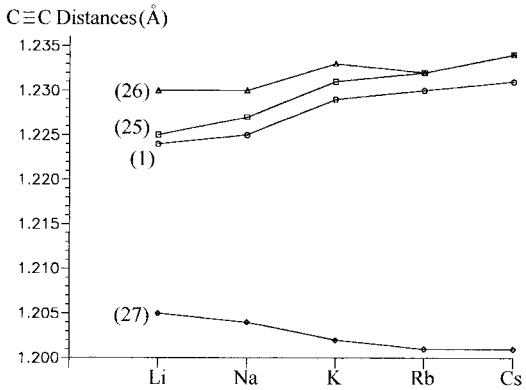

Figure 8. The C≡C distances of the alkali metal acetylene compounds.

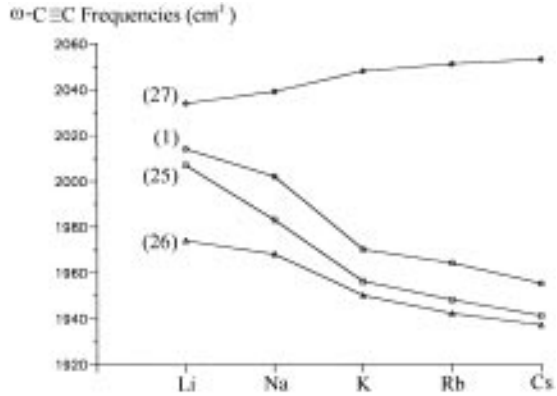

Figure 9. The harmonic ω-C≡C frequencies of the alkali metal acetylene compounds.

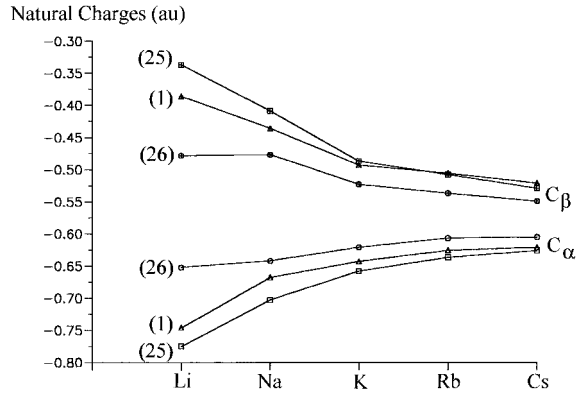

Figure 10. The natural charges on C_α and C_β in the alkali metal acetylides.

$[Me-O-C_6H_4-Si-C{\equiv}C-Si-C_6H_4-O]^+$. Anal. ($C_{11}H_{13}O_1Li_1Si_1$). Calcd: C, 67.3; H, 6.6. Found: C, 66.8; H, 6.8. Single crystals of **14** were obtained from cooled hexane solutions.

X-ray crystal data for $(\mathbf{14})_6$: M_r = 196.24; rhombohedric; space group R-3; $a = b$ = 22.577(3) Å, c = 12.774(2) Å; V = 5638.8(14) $Å^3$; D_{calc} = 1.040 Mgm^{-3}; Z = 18; $F(000)$ = 1872; Mo $K\alpha$ (λ = 0.71073 Å); T = 293 (2) K; crystal dimensions: 0.30 × 0.20 × 0.20 mm; total reflections 2137; unique 1966; $I > 2\sigma(I)$, 1009; parameters, 128. Final R values: $R1$ = 0.0917 ($I > 2\sigma(I)$) and $wR2$ = 0.1759 (all data). GOF = 1.148; largest peak (0.171 e $Å^{-3}$) and hole (−0.150 e $Å^{-3}$).

Li−O−CMe$_2$−C≡C−H (22). A solution of 0.223 g (2.66 mmol) of 2-methyl-3-butyn-2-ol ($H-C{\equiv}C-CMe_2-OH$) in 10 mL of hexane

was cooled to 0 °C and 1.66 mL (2.66 mmol) of 1.6 M BuLi in hexane were added. The white suspension (isolated: 0.23 g, 2.56 mmol, 96% yield), stirred at room temperature for 5 min, dissolved on warming. Slowly cooling to room temperature afforded colorless crystals. NMR of **22**: δ ^{1}H ($CDCl_3$, +25 °C) 2.35 (s, $H-C\equiv C$), 1.44 (s, CH_3); δ $^{13}C\{^1H\}$ ($CDCl_3$, +25 °C) 94.57 (C_1), 67.67 (C_3), 64.51 (C_2), 35.06 (CH_3); IR (Nujol, cm^{-1}) 3270 (ν C−H); MS (EI, 70 eV, 80 °C) *m/e* 457 [M_5-Li^+], 399 [$457^+ - COMe_2$], 341 [$399^+ - COMe_2$]. Anal. ($C_5H_7Li_1O_1$). Calcd: C, 66.7; H, 7.8. Found: C, 66.4; H, 7.9. Single crystals of **22** were obtained from cooled hexane solutions.

X-ray crystal data for $(\mathbf{22})_6$: $M_r = 90.05$; rhombohedral, obv.; space group R-3; $a = b = 10.767(2)$ Å, $c = 26.933(3)$ Å, $V = 2704.0(9)$ Å^3; $D_{calc} = 0.995$ Mgm^{-3}; $Z = 18$; $F(000) = 864$; Mo Kα ($\lambda = 0.71073$ Å); $T = 293$ (2) K; crystal dimensions: 0.30 × 0.30 × 0.20 mm; total reflections 1438; unique 1234; $I > 2\sigma(I)$, 700. H_3 was refined independently and anisotropically; the other hydrogen atoms were fixed in idealized positions using a riding model. Final R values: $R1 = 0.0781$ ($I > 2\sigma(I)$) and $wR2 = 0.1882$ (all data). GOF = 1.185; largest peak (0.192 e Å^{-3}) and hole (−0.155 e Å^{-3}).

Theoretical Section

All computed structures were optimized with Becke's three-parameter hybrid functional[41] incorporating the Lee−Yang−Parr correlation functional[42] (Becke3LYP) using the gradient techniques implemented in GAUSSIAN94.[43] The 6-311+G** (C, H, Li) and 6-31G (Li, Na) basis sets were used. For K, Rb, and Cs 9-valence electron effective core potentials and the LanL2DZ basis sets [*K*, (341/311); Rb, (341/321); Cs, (341/321)] were employed.[44] The character of the stationary points, the zero-point energy correction, and the harmonic vibration frequencies were obtained from analytical and, for pseudo-potential computations of the K, Rb, and Cs systems, from numerical frequency calculations. All partial charges are based on Natural Population Analysis (NPA)[45] of the Becke3LYP electron density. The electrostatic potentials were evaluated with RHF/6-31+G* wave functions on optimized B3LYP geometries.

Acknowledgment. This work was supported by the Fonds der Chemischen Industrie (also through a scholarship to B.G.), the Stiftung Volkswagenwerk, the Convex Computer Corporation, and the Deutsche Forschungsgemeinschaft.

Supporting Information Available: Tables giving crystal data and structure refinement details, atomic coordinates, bond distances and angles, and thermal parameters for **14** and **22** (12 pages). See any current masthead page for ordering and Internet access instructions.

JA9622517

(41) Becke, A. D. *J. Chem. Phys.* **1993**, *98*, 5648.
(42) Lee, C.; Yang, W.; Parr, R. G. *Phys. Rev. B* **1988**, *37*, 785.
(43) GAUSSIAN94, Revision C.3: Frisch, M. J.; Trucks, G. W.; Schlegel, H. B.; Gill, P. M. W.; Johnson, B. G.; Robb, M. A.; Cheeseman, J. R.; Keith, T.; Petersson, G. A.; Montgomery, J. A.; Raghavachari, K.; Al-Laham, M. A.; Zakrzewski, V. G.; Ortiz, J. V.; Foresman, J. B.; Cioslowski, J.; Stefanov, B. B.; Nanayakkara, A.; Challacombe, M.; Peng, C. Y.; Ayala, P. Y.; Chen, W.; Wong, M. W.; Andres, J. L.; Replogle, E. S.; Gomperts, R.; Martin, R. L.; Fox, D. J.; Binkley, J. S.; Defrees, D. J.; Baker, J.; Stewart, J. P.; Head-Gordon, M.; Gonzalez, C.; Pople, J. A. Gaussian, Inc.: Pittsburgh, PA, 1995.
(44) Hay, P. J.; Wadt, W. R. *J. Chem. Phys.* **1985**, *82*, 299.
(45) (a) Reed, A. E.; Curtiss, L. A.; Weinhold, F. *Chem. Rev.* **1988**, *88*, 899. (b) Reed, A. E.; Schleyer, P. v. R. *J. Am. Chem. Soc.* **1990**, *112*, 1434.
(46) Goubeau, J.; Breuer, O. *Z. Anorg. Allg. Chem.* **1961**, *310*, 110.